JOURNAL OF AIRCRAFT
Vol. 29, No. 2, March–April 1992

Effect of Wind Shear on Airspeed During Airplane Landing Approach

Roland J. White*
Boeing Company, Seattle, Washington 98124

Equations are presented for calculating the gust velocity along the landing flight path of an airplane due to the presence of wind shear. Based on this gust input data, airplane equations of motion are solved to determine the minimum airspeed developed during trimmed flight along the landing flight path. Using the developed gust equations, it is shown that the use of a tilted vortex pair provides an improved agreement with measured wind shear velocities. Here, a longitudinal velocity ratio is defined along with a selected vortex core radius. The nonlinear gust velocities are then approximated by a broken line linear ramp gust to use as input gust data for the airplane equations of motion. From this, the minimum airspeed is found along with the flight-path position.

Nomenclature

$A_{()}$ = horizontal velocity coefficients
Au(s) = airplane u velocity transfer function
Au(t) = airplane u velocity time response
a = horizontal vortex distance, ft
$B_{()}$ = vertical velocity coefficients
b = vertical vortex distance, ft
C = vortex core radius, ft/H_s
C_D = airplane drag coefficient
C_L = airplane lift coefficient
C_o = vortex core radius, ft
D = vertical vortex dimension, ft/H_s
FU_o = velocity coefficient
G = glide angle, deg
Gu(s) = longitudinal gust velocity transfer function
Gu(t) = longitudinal gust velocity time response
g = acceleration of gravity
H = altitude, h/H_s
H_o = glide path altitude at $X/R = 1.0$, ft/H_s
H_s = rms gust wave length, ft
h = altitude, ft
L = Von Karman power spectra density scale length, ft
N_{oo} = linear representation factor
P = glide path altitude, ft/H_s
R = vortex pair radius, R_o/H_s
R_o = vortex pair half-spacing, ft
$R_{()}$ = velocity coefficients
r = vortex radius, ft
s = Laplace transfer function variable
t = time, s
t_o = position for $t = 0$
$t(n)$ = time array, s
U_o = airplane trim speed, ft/s
U_1 = airplane speed used for frozen field gust calculation, ft/s
U_T = true airspeed change, kt
U_{ts} = total stall speed change, kt
u = longitudinal gust velocity, ft/s
u_o = vortex pair movement velocity
v_o = vortex tangential velocity, ft/s
WSA = average wind shear, kt/s
WS(n) = wind shear coefficient, kt/s
w = vertical gust velocity, ft/s
X = horizontal ground axis, ft/H_s
x_o = vortex position, ft
z_o = vortex position, ft
α = airplane damping coefficient
β_o = airplane undamped frequency
β = airplane Phugoid frequency
θ = airplane pitch angle
$\theta(s)$ = airplane pitch angle transfer function
κ = vortex circulation, ft²/s
σ_w = rms vertical gust velocity, kt or ft/s
τ = vortex pair tilt angle, deg

Received July 11, 1990; presented as Paper 90-2838 at the AIAA Atmospheric Flight Mechanics Conference, Portland, OR, Aug 20–22, 1990; revision received Nov. 7, 1990; accepted for publication May 29, 1991.

*Retired 1985; currently, Contract Engineer. Senior Member AIAA.

Introduction

In recent years, wind shear has been recognized as the gust velocity produced by a microburst. This has led to the three-dimensional flow analysis developed by vortex rings. These wind shear models have produced suitable nonlinear flow representation for use in flight simulators.[1-3] The present analysis will develop a wind shear gust model to provide coefficients for use with linear airplane stability and control equations.

The present analysis will represent wind shear on a two-dimensional flow basis. This is done by representing the vortex ring as a horizontal vortex pair, having a tilt angle as well as a defined core radius. The vortex pair is located above a defined airplane flight path. From this, the longitudinal gust velocity along the flight path is calculated. This nonlinear velocity is then approximated by a linear gust representation suitable for use in the linear stability equation of motion.

The airplane is then considered to be in trimmed flight during the longitudinal gust encounter, which determines the minimum flight speed reached. If the stall speed is reached, the distance above the ground is noted, which determines the extent of any aviation hazard.

Vortex Pair Wind Shear Model

Wind shear velocity components are calculated based on a vortex pair, along with its image vortices. The strength of the vortices will be taken proportional to the rms vertical gust velocity σ_w. The two-dimensional velocity components then become the sum of the velocities produced by four single vortices to form a nonlinear velocity representation of wind shear.

The single vortex shown in Fig. 1 is defined by its position x_o, z_o along with its circulation κ where

$$\kappa = 2\pi r v_o \tag{1}$$

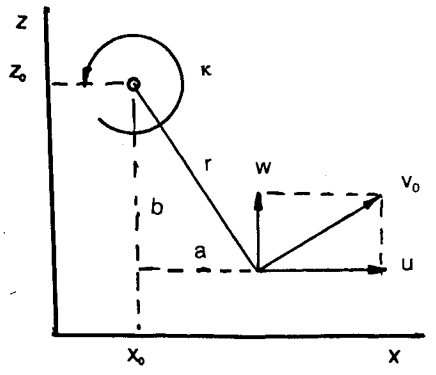

Fig. 1 Vortex velocity components.

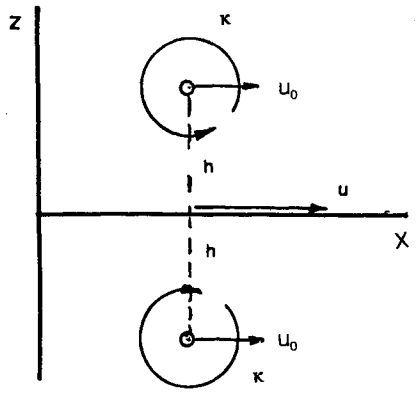

Fig. 2 Vortex side velocity.

This permits the tangential fluid velocity v_o to be calculated for the circular streamline having a radius r. Here

$$v_o = \frac{\kappa}{2\pi r} \tag{2a}$$

$$r^2 = a^2 + b^2 \tag{2b}$$

Noting that the a,b,r dimensions triangle of Fig. 1 is similar to the u,w,v_o velocity triangle permits the velocity components to be written as

$$u = \frac{\kappa}{2\pi r}\left(\frac{b}{r}\right) = \frac{\kappa}{2\pi}\left(\frac{b}{a^2 + b^2}\right) \tag{3a}$$

$$w = \frac{\kappa}{2\pi r}\left(\frac{a}{r}\right) = \frac{\kappa}{2\pi}\left(\frac{a}{a^2 + b^2}\right) \tag{3b}$$

This then permits the velocity at any point in the x,z plane to be calculated based on its geometrical position.

Next, hydrodynamic theory states that the vortex must move with the fluid. Figure 2 shows a vortex along with its image vortex. Here, both vortices produce u as shown based on the previous equations giving

$$u = 2\left(\frac{\kappa}{2\pi h}\right) \tag{4}$$

In addition, both vortices must rotate in the streamline produced by the other vortex. Here

$$u_o = \frac{1}{2}\left(\frac{\kappa}{2\pi h}\right) \tag{5}$$

where u_o represents the side movement of the vortex pair along the x axis. If the other vortex pair has the same value of h but opposite sign, then u_o values cancel each other, giving $u_o = 0$. On this basis, the side velocity movement of the vortex system will occur only for a tilted vortex pair.

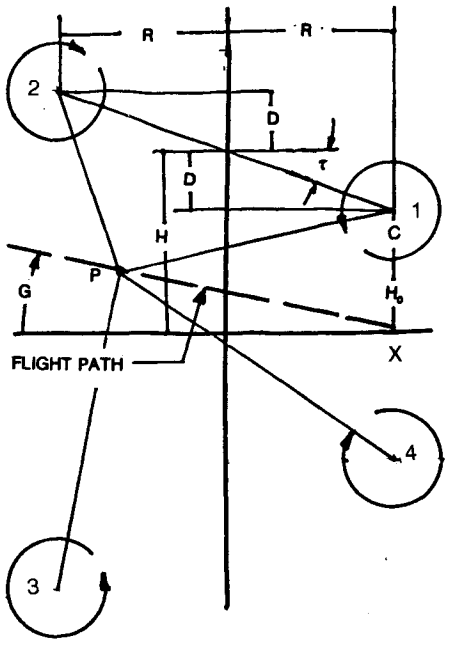

Fig. 3 Wind shear model dimensions.

The next step is to establish a value for the vortex circulation κ. In Ref. 5, based on the Von Karman power spectra density (psd) equation

$$\kappa = 2\pi H_s \sigma_w \tag{6}$$

where the rms gust wave length H_s is taken as $\frac{1}{4}$ of the spectra scale length. For the standard spectra scale length of $L = 2500$ ft, $H_s = 625$ ft. Here, σ_w is the vertical rms gust velocity in feet per second.

In order to represent the gust velocity components in terms σ_w, all linear dimensions in feet are divided by $H_s = 625$ ft. It will be shown that the u and w velocities will then be able to be evaluated in terms of σ_w. Linear dimensions in the following figures and equations will be divided by H_s and upper case characters will be used to represent them.

The wind shear gust velocities may now be calculated along the flight path. Let

$$P = (R - X)\tan G \tag{7a}$$

$$D = R \tan \tau \tag{7b}$$

$$H = C + D + H_o \tag{7c}$$

the $B_{(\,)}$ values for each vortex of Fig. 3, which correspond to the b value of Fig. 1, become

$$B_1 = H - D - P \tag{8a}$$

$$B_2 = H + D - P \tag{8b}$$

$$B_3 = H + D + P \tag{8c}$$

$$B_4 = H - D + P \tag{8d}$$

along with the corresponding $A_{(\,)}$ values of

$$A_1 = X - R \tag{9a}$$

$$A_2 = X + R \tag{9b}$$

$$A_3 = X + R \tag{9c}$$

$$A_4 = X - R \tag{9d}$$

which permit the values of $R_{(\ )}$ to be calculated

$$R_1^2 = B_1^2 + A_1^2 \tag{10a}$$

$$R_2^2 = B_2^2 + A_2^2 \tag{10b}$$

$$R_3^2 = B_3^2 + A_3^2 \tag{10c}$$

$$R_4^2 = B_4^2 + A_4^2 \tag{10d}$$

The velocities at any given point produced by all of the vortices now become

$$\frac{u}{\sigma_w} = + \frac{B_1}{R_1^2} - \frac{B_2}{R_2^2} - \frac{B_3}{R_3^2} + \frac{B_4}{R_4^2} - FU_o \tag{11a}$$

$$\frac{w}{\sigma_w} = - \frac{A_1}{R_1^2} - \frac{A_2}{R_2^2} + \frac{A_3}{R_3^2} + \frac{A_4}{R_4^2} \tag{11b}$$

where

$$\frac{FU_o}{\sigma_w} = \frac{D}{H^2 - D^2} \tag{12}$$

The FU_o coefficient is due to the vortex pair movement, which causes a small change in the frozen field reference speed.

Figure 3 defines the vortex pair position at a height H, with a tilt angle τ, along with a vortex pair spacing of $2R$. In addition, a vortex core radius C is also specified, along with the necessary image vortices.

The landing flight path is also shown in Fig. 3. Here, the vortex pair is assumed positioned to produce a maximum change in the longitudinal gust velocity along the flight path, which occurs when $X = R$. Then, for an average flight-path angle of G, the most critical wind shear will occur when the right vortex core radius is at the runway touch down point, with the left vortex core radius on the flight path.

Figure 4 defines the wind shear model, in nontechnical terms, as having a skate board concept. Here, the vortex pair core radius form the wheels, which must never go beneath the ground level. Next, because the longitudinal wind shear velocity will be greater for lower H values, at least one pair of wheels should be in contact with the flight path in order to produce a large longitudinal gust velocity.

The vortex pair tilt angle τ is determined by a longitudinal velocity ratio (LVR). This ratio as defined here is the absolute value of the exit maximum longitudinal gust velocity divided by the maximum entrance value. The value of LVR may be evaluated from wind shear gust measurements or may be calculated for specified values of τ. Figure 5 shows values of LVR for different tilt angles for two R_o values. Values of FU_o from Eq. (12) are shown in Fig. 6.

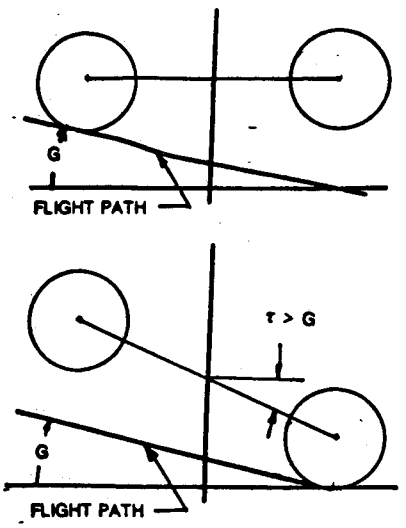

Fig. 4 Skate board concept for wind shear model.

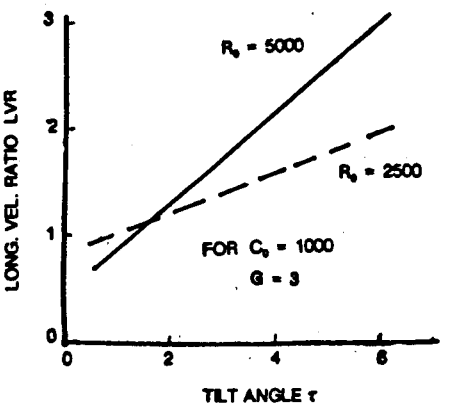

Fig. 5 LVR relationship to tilt angle based on skate board concept.

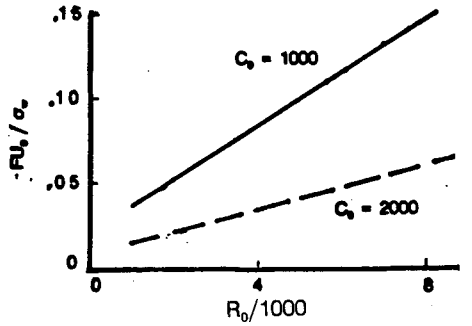

Fig. 6 Vortex pair side velocity.

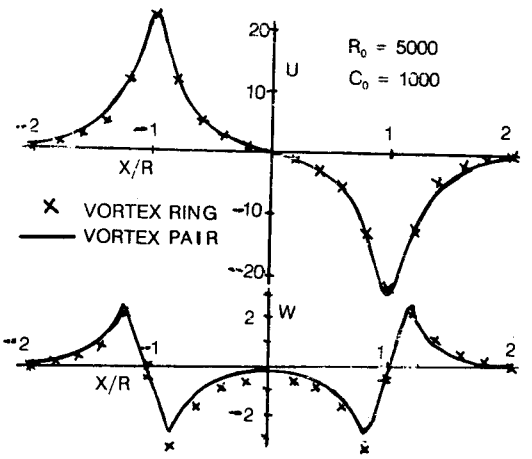

Fig. 7 Present velocity components compared with those for a vortex ring.

Next, sample calculations using the present gust equation will be made, and the results will be compared with those calculated for a vortex ring based on equations of Ref. 3.

The example selected will use $R_o = 5000$ ft, $C_o = 1000$ ft, $\sigma_w = 22.5$ kt, and $\tau = 0$. A level flight path is defined as $H_o = 250$ ft and $G = 0$ deg.

The vortex ring equation of Ref. 3 will require using the vortex pair circulation given by Eq. (6) and setting the y component as defined in Ref. 3 equal to zero. Here, a single ring vortex along with its image is used.

The resulting calculated gust velocity components are shown in Fig. 7. Here, a very good agreement is shown. It should be noted that only a comparison with zero tilt angle can be made because equations in Ref. 3 do not include this variable.

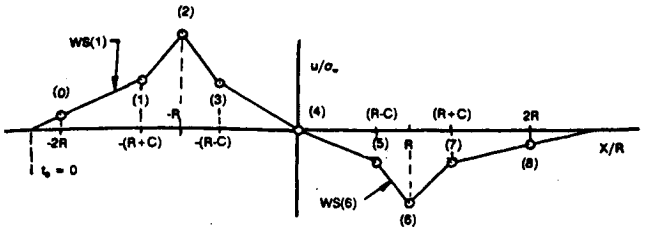

Fig. 8 Specified array numbers for selected wind shear break points.

Linear Representation of Gust Velocities

It is now desired to represent these velocities by a linear slope between specific points to provide gust input coefficients for use with the linear stability and control equations.

Figure 8 shows the specified points to be calculated, which will form the stability equation input coefficients, along with specified break points for the solution of the differential equations.

As explained in Ref. 4, the frozen field concept is used to represent the gusts. If a gust tilt angle τ occurs, then the frozen field reference speed is different from the airplane trim speed. If U_o represents the airplane trim speed, then the frozen field reference speed U_1 is

$$U_1 = U_o - FU_o\sigma_w \tag{13}$$

Here, the FU_o term from Eq. (12) is used in calculating U_1, which permits dropping this term from Eqs. (11). This then permits a time for each point to be specified based on

$$t = \left(\frac{X}{R} + 2\right)\frac{R_o}{U_1} + t_o \tag{14}$$

where t_o is equal to zero, as noted in Fig. 8.

In order to provide a better linear fit to the slopes in Fig. 8, calculated values at points 1, 3, 5, and 7 were reduced by a factor N_{oo} where

$$N_{oo} = 1 - 0.25\left(\frac{R_o}{5000}\right) \tag{15}$$

The final coefficients for use in the differential equations now become

$$t(n) = \left(\frac{X}{R} + 2\right)\frac{R_o}{U_1} + t_o \tag{16a}$$

$$\mathrm{WS}(n) = \frac{\mathrm{Gu}(n) - \mathrm{Gu}(n-1)}{t(n) - t(n-1)} \tag{16b}$$

Airplane Motion Gust Response

The longitudinal gust velocity data shown in Fig. 8 become the input data necessary to calculate the change in the airplane airspeed.

The airplane equations of motion used to represent the airplane are the Phugoid equations given in Chapter VI of Ref. 4. These equations permit the airplane speed change Au along with the change in airplane pitch angle θ to be calculated. Here

$$\alpha = \frac{C_D g}{C_L U_1} \tag{17a}$$

$$\beta_o = \frac{\sqrt{2}g}{U_1} \tag{17b}$$

$$\beta^2 = \beta_o^2 - \alpha^2 \tag{17c}$$

These coefficients are used in the airplane transfer functions to be evaluated. Here α represents the airplane Phugoid motion damping, and β the corresponding frequency.

The gust and airplane Laplace transfer functions are

$$\mathrm{Gu}(s) = \frac{\mathrm{WS}(1)}{s^2} \tag{18a}$$

$$\mathrm{Au}(s) = \frac{-\mathrm{WS}(1)(2\alpha s + \beta_o^2)}{s^2(s^2 + 2\alpha s + \beta_o^2)} \tag{18b}$$

Then, with a partial fraction expansion

$$\mathrm{Au}(s) = \frac{-\mathrm{WS}(1)}{s^2} + \frac{\mathrm{WS}(1)}{s^2 + 2\alpha s + \beta_o^2} \tag{19}$$

the corresponding pitch angle transfer function is

$$\theta(s) = \frac{\mathrm{WS}(1)\left(\frac{\beta_o^2}{g}\right)}{s(s^2 + 2\alpha s + \beta_o^2)} \tag{20}$$

The actual total airspeed change experienced along the flight path is the sum of Au(t) + Gu(t) time response. Then, from the transfer functions

$$\mathrm{Gu}(t) = \mathrm{WS}(1)t \tag{21a}$$

$$\mathrm{Au}(t) = -\mathrm{WS}(1)t + \left(\frac{\mathrm{WS}(1)}{\beta}\right)e^{-\alpha t}\sin\beta t \tag{21b}$$

$$\theta(t) = \frac{\mathrm{WS}(1)}{g}\left(1 + \frac{\beta_o}{\beta}\right)e^{-\alpha t}\sin\left[\beta t - \tan^{-1}\left(\frac{\beta}{-\alpha}\right)\right] \tag{21c}$$

giving

$$U_T = \mathrm{Gu}(t) + \mathrm{Au}(t) \tag{22a}$$

$$U_T = \left(\frac{\mathrm{WS}(1)}{\beta}\right)e^{-\alpha t}\sin\beta t \tag{22b}$$

where U_T is the actual change of the longitudinal airspeed during the landing approach.

Example Calculations

Calculations are made to determine the minimum airspeed reached during the landing approach using the present wind shear equations. Airplane data used is that for the general aviation airplane D, as presented in Ref. 4. Here, for the power approach condition for trim at 1.30 V_s

$$U_o = 170 \text{ ft/s} \tag{23a}$$

$$C_L = 1.64 \tag{23b}$$

$$C_D = 0.256 \tag{23c}$$

Using these data, a $C_{L\,\max} = 2.77$ was estimated to match the calculated drag equation

$$C_D = 0.044 + 0.079\,C_L^2 \tag{24}$$

A flight-path glide angle of 3 deg will be assumed. The airplane is considered in trim for the 3.0-deg glide slope. Here

$$\frac{C_D}{C_L} = \tan 3.0 = 0.0524 \tag{25}$$

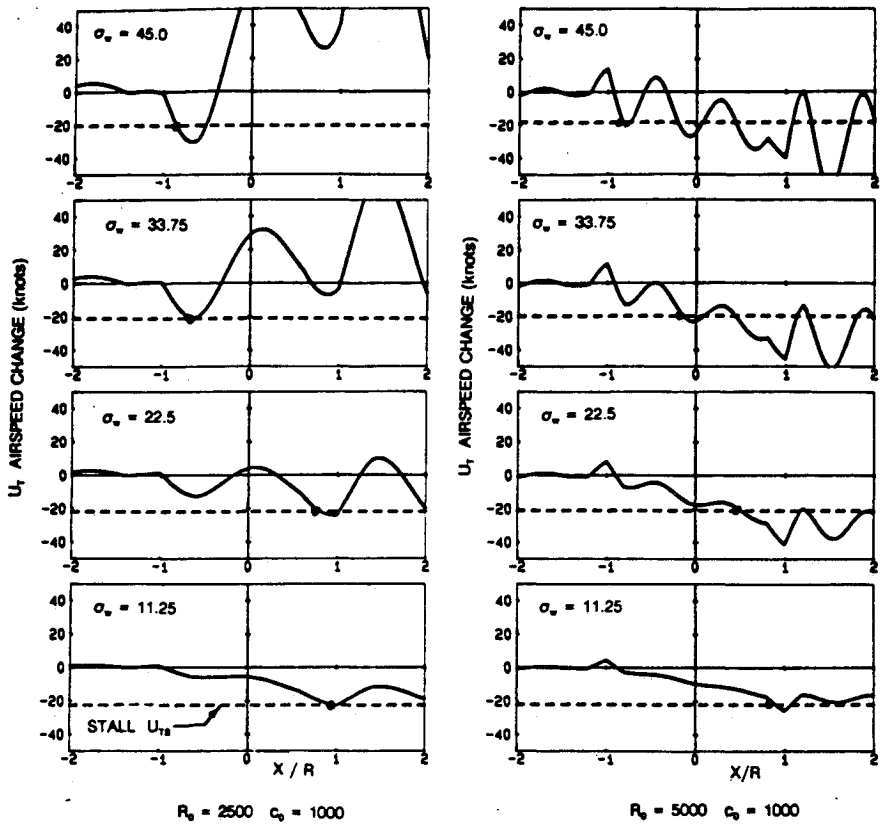

Fig. 9 Airplane total airspeed change.

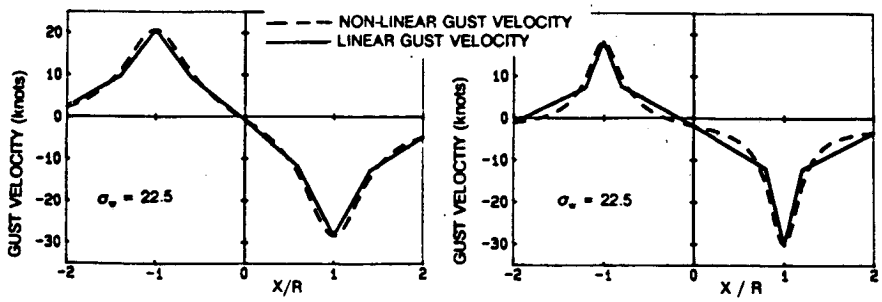

Fig. 10 Corresponding longitudinal gust velocity.

giving $C_D = 0.0900$, which includes thrust effects and is maintained through use of engine thrust.

Then, based on Eq. (25), values of the airspeed change U_T are calculated for four different values of σ_w and two values of R_o. The results of these calculations are plotted in Fig. 9.

The estimated stall speed change is also shown on each of the plots of Fig. 9 based on the equation

$$U_{ts} = \frac{U_1 - U_o/1.3}{1.689} \tag{26}$$

where the approach speed is 30% above stall speed.

The crossover points, as noted in Fig. 9, permit the airplane stall position along the airplane approach path to be determined.

Figure 10 shows a comparison of the linear and nonlinear gust velocities for the same two values of R_o used in Fig. 9 with $C_o = 1000$ ft.

From this, the final desired results are calculated and presented in Fig. 11. Here, the stall altitude is shown along with an average wind shear value (WSA) given in knots per second. The calculated stall altitude represents a worst case solution. Here, the wind shear is acting at the minimum possible altitude to give the maximum longitudinal gust velocity. The airplane power trim setting is maintained with fixed flight controls.

The average wind shear quantity WSA is suggested as a wind shear reference value. This value is based on the time to reach airplane stall T_s minus T_2, which is when the maximum gust Gu(2) starts to reduce.

To make comparisons, a σ_w value should be selected. If it is assumed that the maximum horizontal rms velocity for severe thunderstorm weather is 45 kt at sea level, then for the present analysis, which includes ground effects, half of this value should be the velocity at altitude.

Table 1 compares the WSA value with the initial calculated value WS(1) and the greatest negative value WS(6). These data are for $\sigma_w = 22.5$ kt, which represents the approximate vortex ring wind shear for severe thunderstorm weather.

The WSA reference value of Table 1 permits a comparison with other wind shear calculations, such as those of Ref. 6 that describe the wind shear effect on the airplane motion in terms of the airplane performance equations.

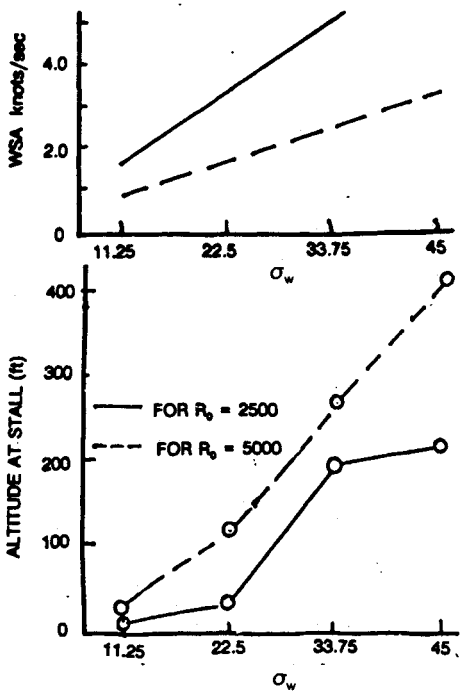

Fig. 11 Estimated stall altitude for example airplane.

Table 1 Wind shears for σ_w = 22.5 kt

	R_o = 2500 ft, kt/s	R_o = 5000 ft, kt/s
WSA	3.27	1.57
WS(1)	0.82	0.35
WS(6)	−2.74	−2.98

Discussion

Example calculations based on the present equations were made for R_o = 2500 and 5000 ft using a core radius C_o = 1000 ft. Here, different values of σ_w were used.

Figure 9 shows the position along the glide path where the airplane stall occurs. For small values of σ_w, the stall first occurs at or near X/R = 1, which is the glide path touch down point. As σ_w is increased, the stall occurs sooner and at a higher glide altitude. The stall altitude calculated from the crossover points of Fig. 9 are shown plotted in Fig. 11 along with the average wind shear values.

All of the present calculations were made to demonstrate how the nonlinear wind shear gust model may be used with the airplane linear stability and control equations involving pilot flight controls. Here, only trimmed flight was considered at the lowest possible vortex altitude.

The introduction of LVR as a wind shear gust parameter is important because of the gust ground effects. Figure 10 shows the nonlinear longitudinal gust velocity along with the linear approximation used in the present example calculations.

The calculation of LVR in terms of the vortex pair tilt angle τ is important, as it permits a more accurate representation of the wind shear velocity. The need for a discrete type of gust wind shear model is desired for the study of wind shear detection and avoidance methods.

Conclusions

Equations showing the wind shear effect are presented for the airplane in landing approach flight. These two-dimensional gust equations approximate the nonlinear wind shear velocities by a broken line linear ramp gust. This is done by defining the wind shear gust in terms of an equivalent vortex pair having a radius R_o, a vortex core radius c_o, and a tilt angle τ. The use of the vortex pair tilt angle τ is shown to improve the gust representation of wind shear.

It is shown that a standard wind shear discrete gust representation is possible if the gust break points of Fig. 8 are specified. This would form the gust data input for linear airplane equations representing the pilot control operations. The value of the vortex pair tilt angle may be caluclated from wind shear velocity test data using the measured value of LVR. The determination of R_o and c_o may also be found from the test data to give the best longitudinal velocity representation.

References

[1]Fujita, T. T., *DFW Microburst*, University of Chicago Press, Chicago, IL, 1986.

[2]Michael, I., "A Ring-Vortex Downburst Model for Flight Simulation," *Journal of Aircraft*, Vol. 23, No. 3, 1985, pp. 232–236.

[3]Schultz, T. A., "A Multiple-Vortex Ring Model of the DFW Microburst," AIAA Paper 88-0685, 1988, pp. 1–8.

[4]Roskam, J., "Airplane Flight Dynamics and Automatic Flight Controls," Roskam Aviation Co., 1982, pp. 428–433.

[5]White, R. J., "A Wind Shear Gust Model Useful in Evaluating Airplane Flying Qualities," *Proceedings Techfest XV*, 1988.

[6]Wattson, R., Jr., "Impact of Wind Shear on Airplane Performance," *Proceedings Techfest XV*, 1988.